Fracture Mechanics of Concrete Structures,
Proceedings FRAMCOS-2, edited by Folker H. Wittmann,
AEDIFICATIO Publishers, D-79104 Freiburg (1995)

RUPTURE MODULUS AND FRACTURE PROPERTIES OF CONCRETE

J. Planas, G. V. Guinea and M. Elices
Departamento de Ciencia de Materiales, ETS de Ingenieros de Caminos,
Universidad Politécnica de Madrid, Spain.

Abstract
This paper analyzes the approaches of various authors to the size effect on the rupture modulus and compares the predictions of the models to each other and to some of the available experimental results. Closed form analytical expressions are given for the modulus of rupture predicted by Hillerborg's cohesive crack model, the Bazant-Li boundary layer model and the Jenq-Shah two parameter model; the multifractal scaling law of Carpinteri, Chiaia and Ferro is also analyzed.

1 Introduction

The modulus of rupture, measured for beams in either three or four point bending, provides a measure of the strength of a brittle or quasi-brittle material that is experimentally convenient because the tests are relatively easy to carry out. This was recognized and various standard procedures for such tests are available.

Unfortunately, the modulus of rupture does not in general coincide with the tensile strength, as is recognized, for example, by the ACI code that assumes that, on average, the rupture modulus f_r is 25 % higher than f_t, the tensile strength. However, the problem is not reduced to such a simple relationship, because it is widely accepted that the modulus of rupture is size dependent.

The size dependence of the modulus of rupture has been experimentally demonstrated many times (Reagel and Willis 1931; Wright 1952; Nielsen 1954; Lindner and Sprague 1953; Walker and Bloen 1957; Petersson 1981; Alexander 1987; Elices, Guinea and Planas 1994) and has been incorporated, for example, into the CEB-FIP Model Code (1990). To justify and evaluate such size effect, various theories have been used. The earliest theories were based on the statistic approach of Weibull (1939) developed for brittle materials whose strength is totally dependent on the characteristics of the worst flaw (weakest link theory). However, it turned out later that this theory is not directly applicable to concrete because in concrete many initial flaws grow and coalesce before the peak load is reached. This is not to say that concrete is immune to statistical size effect; of course it is not, but the dependence is milder than for brittle materials with single-flaw failure, and in many cases the fracture mechanics size effect dominates (see, e.g., Bazant, Xi and Reid 1991).

This paper reviews various deterministic theories developed to explain the size effect on the modulus of rupture, all based on more or less simplified nonlinear fracture models. After introducing the notation and common equations (§2), we start describing the various analyses based on numerical computations according to the cohesive or fictitious crack model proposed for concrete by Hillerborg (§3). This includes new closed-form expressions that depend only on the initial portion of the softening curve. Next, the predictions of the rupture modulus by other models are briefly reviewed and compared with those of the cohesive crack model: the boundary layer model of Bazant and Li (§4.1), the two parameter model of Jenq and Shah (§4.2) and the recent multifractal scaling law of Carpinteri Chiaia and Ferro (§4.3) are the models investigated. The paper closes by comparing the various approaches with some experimental results.

2 Notation and definition of the rupture modulus

For bending, either three or four point (Fig. 1), the nominal stress is conveniently defined as

$$\sigma_N = \frac{6M}{BD^2} \tag{1}$$

where M is the bending moment in the central cross-section, B the specimen thickness and D the beam depth. The nominal strength σ_{Nu} is, by definition, the modulus of rupture f_r:

$$f_r = \sigma_{Nu} = \frac{6M_u}{BD^2} \tag{2}$$

where M_u is the ultimate bending moment.

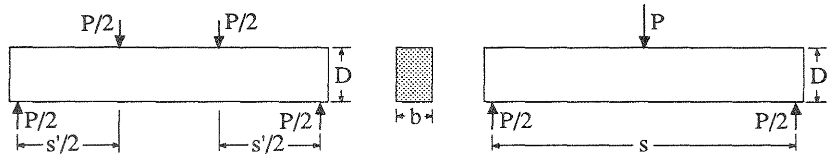

Fig. 1. Four- and three-point bending beams.

The rupture modulus was in its origin assumed to be a material property coincident with the tensile strength. This is basically true for an elastic-brittle material, defined as one that remains elastic until at some point the tensile stress reaches the tensile strength f_t, at which moment catastrophic failure occurs. Then, for pure bending the rupture modulus of an elastic brittle material must coincide with the tensile strength. However, for three point bending, the rupture modulus must be expected to be larger by about 5 % even for an elastic-brittle material. This is so because in three-point bending the stress distribution along the central cross-section is slightly different from that in pure bending. In particular, the maximum elastic tensile stress σ^{el}_{max} is not identical to σ_N (as for pure bending), but is slightly lower. According to Timoshenko and Goodier (1951) the peak stress is given by

$$\sigma^{el}_{max} = \sigma_N \left(1 - 0.1773 \frac{D}{s}\right) \tag{3}$$

where s is the loading span. Thus, for an elastic brittle material the modulus of rupture would be

$$f_r = \beta f_t \quad \text{with} \quad \beta = \frac{1}{1 - 0.1773 D/s} \tag{4}$$

According to this formula, $\beta = 1.046$ for $s/D = 4$. Gustafsson (1985) numerically found $\beta = 1.053$ for such a case; the authors, using finite elements with 100 equal elements over the central cross-section, found a value coincident within the expected error with the one given by (4), which will be used in the remainder of the paper.

We remark that Gustafsson redefined the modulus of rupture to include the factor β, so that the newly defined rupture modulus would be equal to the tensile strength also for three point bending. Here we stick to the classical definition (2) as used in most standards.

3 Modulus of rupture predicted by cohesive cracks

The analysis of the bending test was one of the early applications of the cohesive or fictitious crack (Hillerborg, Modéer and Petersson 1976). After this initial work, which used linear softening and a relatively coarse finite element mesh, further, more precise computations were performed by Hillerborg and co-workers to disclose the influence of the shape of the softening curve (Modéer 1979) and to examine the influence of shrinkage (Petersson 1981; Gustafsson 1985). The results showed that the rupture modulus was size-dependent and that it also depended, quite sensitively, on the shape of the assumed softening curve.

Many other researchers since, have used the cohesive crack to describe the fracture in bending. In no case, however, is the numerical solution completely consistent with the cohesive crack hypotheses. Indeed, as pointed out, qualitatively, by Hillerborg and co-workers and quantitatively by Olsen (1994), in the computation the tensile strength is exceeded over relatively large regions outside the assumed main crack. This means that secondary cracking *must* occur. This is neglected in the solutions produced so far for the modulus of rupture. Planas and Elices (1993) included the secondary cracking in a relatively simple way for the cases where strong shrinkage is present, a way that can be extended to the no-shrinkage case with additional hypotheses which, however, require relatively sophisticated computations. In the remainder of this paper, all the solutions refer to the classical approximations in which secondary cracking is neglected.

The classical approximations are relatively easy to carry out using the appropriate software. Here we look for closed form formulas relating the numerical solutions to the softening curve of the material, so that these formulas can be used in regression analysis of experimental data.

3.1 Formulas depending on the softening curve

To summarize the results delivered by the numerical results, various formulas have been proposed. Here we summarize those that are softening-dependent, i.e. those including parameters that vary with the shape of the softening curve.

Gustafsson did not produce a general formula for the modulus of rupture, but he derived two asymptotic expressions; he proposed the following formulas for pure bending ($\beta = 1$) and large sizes:

$$\frac{f_r}{f_t} = 1 + \frac{1}{b_1\, D/\ell_{ch}} \qquad \text{(first order approximation)} \qquad (5)$$

$$\frac{f_r}{f_t} = 1 + \frac{1}{1 + b_1\, D/\ell_{ch}} \qquad \text{(second order approximation)} \qquad (6)$$

where b_1 is a dimensionless constant depending on the shape of the softening curve, and ℓ_{ch} is the classical Hillerborg's characteristic size defined as

$$\ell_{ch} = \frac{E G_F}{f_t^2} \qquad (7)$$

where G_F is the fracture energy (the area under the softening curve) and E

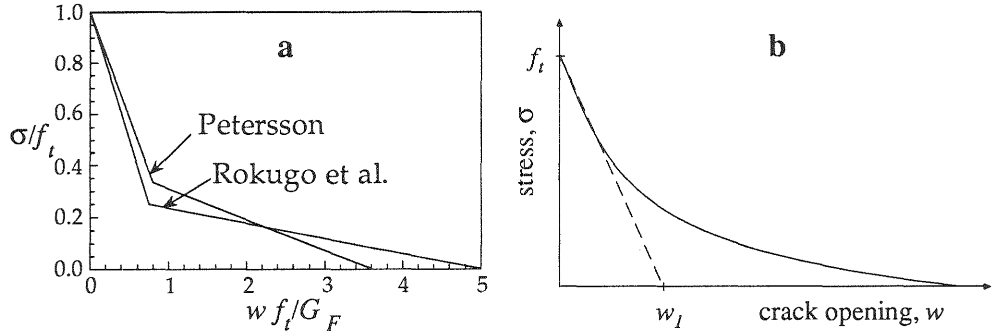

Fig. 2. (a) Bilinear softening curves proposed for concrete by Petersson (1981) and Rokugo et al. (1989). (b) Initial linear approximation (after Planas and Elices 1992).

is the elastic modulus. The value of b_1 for the so called Petersson's bilinear softening depicted in Fig. 2a is 3.7 (Gustafsson 1985).

Recently, Eo, Hawkins and Kono (1994) analyzed again the evolution of the modulus of rupture using bilinear softening curves of various shapes. Their results confirmed that the modulus of rupture depends on the details of the curves. They proposed to fit the results by a modification of the well known Bazant's (1984) size effect law , by adding to it a constant term as follows:

$$\frac{f_r}{f_t} = \frac{B}{\sqrt{1 + D/D_0}} + C \tag{8}$$

where B, D_0 and C are constants to be obtained by curve fitting procedures for each softening. The fits to numerical results obtained by Eo, Hawkins and Kono were excellent over size ranges of 0.1 to 1.5 m. However this curve has three parameters and we shall show below that for cohesive cracks only one parameter should be allowed to vary freely with the softening shape. Moreover, the values obtained for C were around 0.15, which means that for this curve the asymptotic value for $D \to \infty$ is $f_r = 0.15 f_t$, while it is known that the correct asymptotic value for a cohesive crack model is $f_r = f_t$ (for pure bending).

The following formula —with the correct asymptotic behavior for large sizes— was proposed by Uchida, Rokugo and Koyanagi (1992):

$$\frac{f_r}{f_t} = 1 + \frac{1}{b_2 + b_1\, D/\ell_{ch}} \tag{9}$$

where b_1 and b_2 are constants depending on the softening curve. For the bilinear softening curve proposed by Rokugo et al.(1989) and depicted in Fig. 2a, the values $b_1 = 4.5$ and $b_2 = 0.85$ give a good fit of the numerical results for $D \geq 0.1\ \ell_{ch}$ (Uchida, Rokugo and Koyanagi 1992).

3.2 Formulas depending on the initial softening slope

The fact that all the constants in the foregoing fitting equations depend on the details of the shape of the softening curve is a drawback for their generalization. The way towards a formulation independent (in a sense to be made more precise later) of the shape of the softening curve, was opened by Alvaredo and Torrent (1987), who noticed that for bilinear curves the rupture modulus depends only on the initial softening segment, rather than on the whole softening curve. This property was shown by the authors to be extensive to other nonlinear softening curves and to other situations (presence of shrinkage stresses).

The basic result of the analysis of Planas and Elices (1992, 1993) is that the softening curve influences the modulus of rupture only through its initial part, that can, in most cases, be approximated by a straight line, as depicted in Fig. 2b. This means that only two parameters of the softening curve are relevant: the tensile strength f_t and the horizontal intercept of the initial tangent w_1 (Fig. 2b). Thus, from the basic equations governing the cohesive crack growth, it turns out that the relationship between the rupture modulus and the size must take the form

$$\frac{f_r}{f_t} = H(D/\ell_1) \qquad \text{with} \quad \ell_1 = \frac{Ew_1}{2f_t} \tag{10}$$

where $H(D/\ell_1)$ is a dimensionless function that depends implicitly on the kind of loading: three or four point bending, and span-to-depth ratio. ℓ_1 is a characteristic size similar to ℓ_{ch}, except that the area $f_t w_1/2$ of the triangle defined by the axes and the dashed line in Fig. 2b is used instead of G_F, the area under the full curve.

The foregoing property is illustrated in Fig. 3a which shows that when plotted versus D/ℓ_1 the modulus of rupture of the three different softening curves depicted in Fig. 3b (solid curves) do very approximately coincide. We shall discuss in more detail why and for which kind of softening this property holds in §3.3.

A closed form expression for $H(D/\ell_1)$ was sought which can be considered valid for the whole range of sizes, thus satisfying $f_r \rightarrow 3 f_t$ for $D \rightarrow 0$ (plastic limit solution for cohesive cracks), and $f_r = \beta f_t$ for $D \rightarrow \infty$ (Eq. eo4). The expression proposed —a generalization of the Gustafsson expression (6)— is the following:

$$\frac{f_r}{f_t} = \beta + \frac{3\text{-}\beta+99D^*}{(1+2.44D^*)(1+87D^*)}\ , \qquad D^* = \frac{D}{\ell_1} \tag{11}$$

Expressions such as (5), (6) and (9) that use the characteristic size, can be transformed to the softening-independent form (10) making use of the relationship between ℓ_1 and ℓ_{ch}:

$$\ell_1 = \frac{w_1 f_t}{2G_F}\,\ell_{ch} = c_0\,\ell_{ch} \tag{12}$$

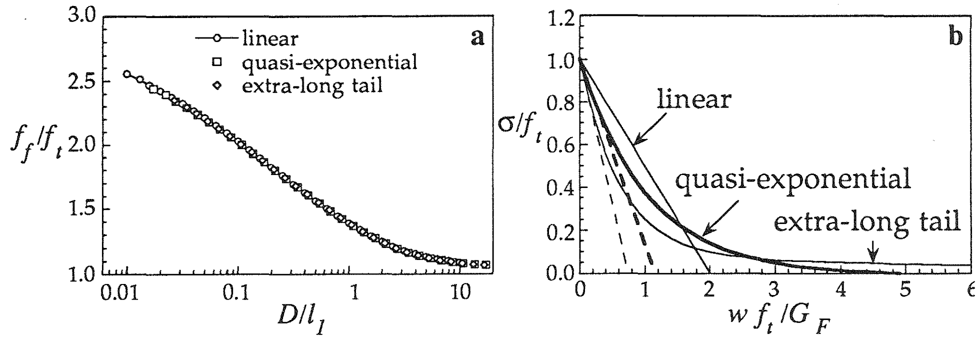

Fig. 3. Size effect curves for the modulus of rupture (a) computed for various softening shapes (b). (After Planas and Elices 1992.).

where, obviously, the factor c_0 depends on the shape of the softening curve. For concrete, c_0 is usually in the range 0.4–0.6 (the smaller the steeper the initial softening). In this way, (5), (6) and (9) can be recast in the general form

$$\frac{f_r}{f_t} = \beta\left(1+\frac{1}{c_2 + c_1\, D/\ell_1}\right) \tag{13}$$

where, for successive approximation levels, the constants take the values

$$\begin{aligned} c_2 &= 0.00, \; c_1 = 2.3 \quad \text{(level I)}\\ c_2 &= 1.00, \; c_1 = 2.3 \quad \text{(level II)}\\ c_2 &= 0.85, \; c_1 = 2.3 \quad \text{(level III)} \end{aligned} \tag{14}$$

Fig. 4a shows the comparison of the numerical predictions of the cohesive model with the expressions (11) and (13)-(14) for three point bending with a span to depth ratio of 4 (β= 1.046). All give a good approximation for large sizes (D>3ℓ_1). The third order approximation gives a very good approximation for D>0.1ℓ_1, a range valid for most practical purposes (for a typical concrete ℓ_{ch} ~ 300 mm, so ℓ_1 ~ 150 mm and 0.1ℓ_1 ~ 15 mm, a very small size for most applications).

3.3 Further analysis of the influence of the initial softening

The idea that the rupture modulus depends only on the initial softening slope was so far based on the examination of a couple of cases for which this happens to be the case. For deeper insight, we should be able to understand why this is so and to define the kind of softening curves that may be expected to satisfy the foregoing formulation.

The main reason seems to be clear: for the bending tests on unnotched specimens, the peak load occurs before any point on the cohesive zone softens very much. This can be verified by recording the amount of softening experimented at peak load by the element situated at the cohesive crack mouth, which is the one experiencing most softening.

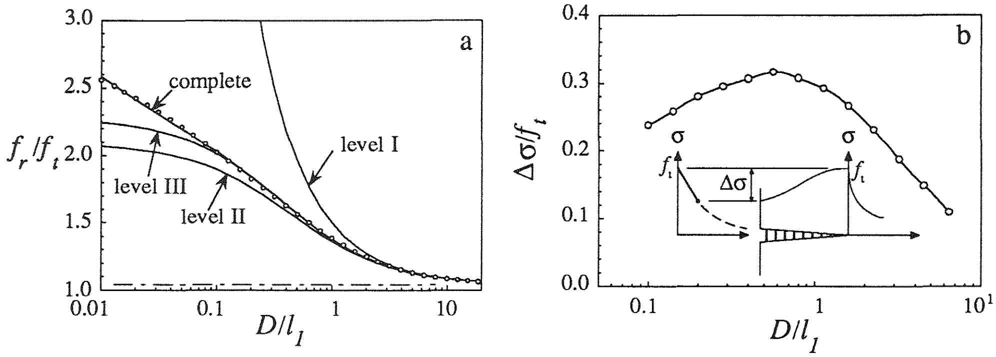

Fig. 4. (a) Computed size effect curve for the modulus of rupture in three-point bending with s/D ratio of 4, and analytical approximations (11)–(13). (b) Stress-softening at the cohesive crack mouth vs. specimen size.

Fig. 4b shows the results for a range of specimen sizes; they indicate that the softening experienced at peak load never exceed 32% of the tensile strength. Therefore, any softening that can be reasonably approximated by a straight segment for stress softenings in the range of cohesive stresses from the maximum (f_t) down to 078f_t is expected to give size effect curves well described by the equations in the foregoing section.

4 Other approximations to the modulus of rupture

4.1 Modulus of rupture according to Bazant-Li model

The approximation of Bazant and Li (1993) is based on the assumption that prior to the peak load, the cracking in concrete is distributed rather than localized (Fig. 5a). The peak load is assumed to occur when the greatest depth of the microcracked zone x reaches a certain critical value ℓ_f. The problem is further simplified by assuming that up to peak the beam can be analyzed by the elementary beam theory (cross-sections remain plane, shear is neglected), and that the uniaxial stress-strain behavior of concrete is elastic with linear softening, as depicted in Fig. 5b.

To obtain the solution, the equilibrium conditions are imposed on the central cross-section for arbitrary x (Fig. 5c) from which an equation relating the bending moment M to x is easily obtained.

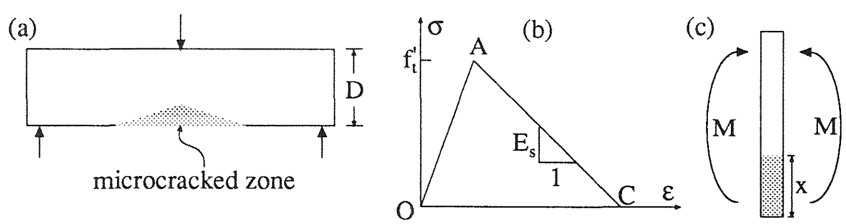

Fig. 5. (a) Microcracked zone in Bazant-Li model. (b) Softening curve. (c) Microcracked zone at the central cross-section

The peak load is obtained by setting, according to the basic hypothesis of Bazant and Li, $x = \ell_f$. From this, the following equation results:

$$\frac{f_r}{f_t} = 1 + 2\,\frac{\ell_f}{D} - \frac{4k}{k+(D/\ell_f - 1)^2} \qquad (15)$$

where

$$k = E_s/E \qquad (16)$$

is the reduced softening modulus (Fig. 5b).

The foregoing is the exact solution of the problem as defined by Bazant and Li (1993), which was not elaborated in their work; Bazant and Li used a truncated series expansion, and suggested that for relatively large sizes ($\ell_f/D \ll 1$) only two terms were sufficient. Since the third term in (15) is quadratic in ℓ_f/D, the size effect proposed by Bazant and Li reads

$$\frac{f_r}{f_t} = 1 + 2\,\frac{\ell_f}{D} \qquad (17)$$

Fig. 6a shows the evolution of the modulus of rupture with size as predicted by the Bazant-Li model. Note that the first order approximation is achieved over most of the range if the value of k is very small (i.e., if the softening is very gradual). For finite values of k, the model predicts a descending branch for small sizes, which is unrealistic.

The Bazant-Li model did not, as initially formulated, take into account the effect of the concentrated load. This can be included by multiplying the right hand side of equation (17) by β. It turns out then that the Bazant-Li asymptotic equation coincides with Gustafsson's first order approximation (5) and its reformulation (13)-(14). Thus, ℓ_f and ℓ_1 can be related so that the asymptotic behavior is coincident; setting the parenthesis in (13) —with c_2=0 and c_1=2.3— equal to (17) we get

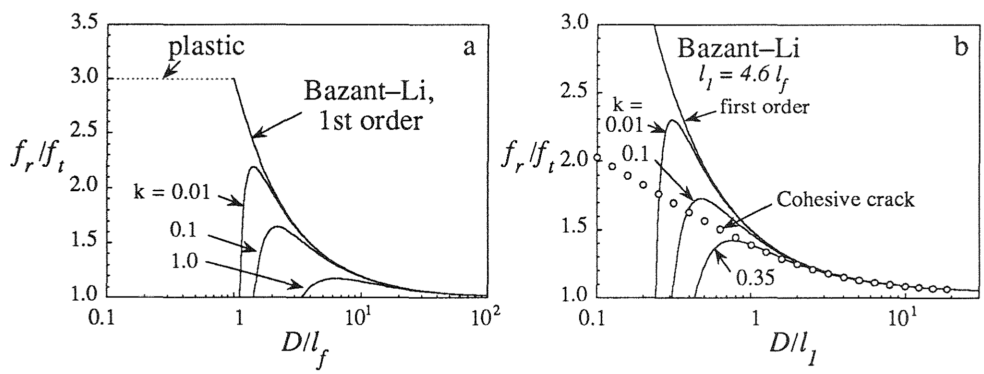

Fig. 6. Evolution of size effect curve according to Bazant-Li model.

$$\ell_f = \frac{\ell_1}{2c_1} = 0.217\,\ell_1 \qquad \text{or} \qquad \ell_1 = 4.6\,\ell_f \tag{18}$$

Fig. 6b compares the predictions of the Bazant-Li and cohesive crack models. Note that selecting an appropriate value for k (≈ 0.35) a very good coincidence is achieved for $D>\approx 0.8\,\ell_1$. If the first order approximation is used (equivalent to $k = 0$) the range over which the two models coincide within 10% is reduced to $D>\approx \ell_1$. However, no good correspondence is found for the small sizes typical of laboratory specimens.

4.2 Modulus of rupture predicted by Jenq-Shah model

The Jenq-Shah model assumes that starting from a preexisting crack, which may be taken to be vanishingly small, a macrocrack grows until the peak load is reached, at which moment both the stress intensity factor K_I and the crack tip opening displacement w_T reach their critical values K_{Ic} and w_{Tc}; the corresponding crack length at the peak is denoted as a_c.

For a vanishingly small initial crack, the stress intensity factor and CTOD can be written as

$$K_I = \sigma_N \sqrt{D}\, S(a/D)\,, \qquad w_T = \frac{\sigma_N}{E'}\, D\, M(a/D) \tag{19}$$

where $S(a/D)$ and $M(a/D)$ are shape functions that have been approximated by closed form expressions for both three point and four point bending (see e.g., Tada, Paris and Irwin 1985 for classical expressions; see Pastor et al. 1995 for enhanced expressions valid for any span-to-depth ratio ≥ 2.5). Particularizing (19) for the peak load condition ($K_I = K_{Ic}$, $w_T = w_{Tc}$, $a=a_c$, and $\sigma_N = f_r$) and assuming that the two material parameters K_{Ic} and w_{Tc} have been determined by other experiments, we get two equations with the two unknowns a_c and f_r which can be solved for f_r for any given size. When we want to obtain the size effect curve, i.e. let D vary, it is better to use $\alpha_c = a_c/D$, D and f_r as variables, so that solving for f_r and D as a function of α_c we get:

$$\frac{D}{\ell_0} = \frac{S^2(\alpha_c)}{M^2(\alpha_c)}\,, \qquad \ell_0 = \frac{E'^2\, w_{Tc}^2}{K_{Ic}^2} \tag{20}$$

$$\frac{f_r}{f_0} = \frac{2M(\alpha_c)}{3S^2(\alpha_c)}\,, \qquad f_0 = 1.5\frac{K_{Ic}^2}{E'\, w_{Tc}} \tag{21}$$

These two equations are the parametric representation of the size effect curve, with parameter α_c. Plotting the pairs (D, f_r) for all α_c, the size effect plot is obtained. This has been done for three-point bending, using the following expressions of $S(\alpha)$ and $M(\alpha)$:

$$S(\alpha) = \sqrt{\alpha}\,\frac{1.9-\alpha\left[-0.089+0.60(1-\alpha)-0.44(1-\alpha)^2+1.22(1-\alpha)^3\right]}{(1+2\alpha)(1-\alpha)^{3/2}} \tag{22}$$

$$M(\alpha) = 4\,\alpha\left[0.76-2.28\,\alpha+3.87\alpha^2-2.04\alpha^3+\frac{0.66}{(1-\alpha)^2}\right] \tag{23}$$

The expression for $M(\alpha)$ has been taken from Tada, Paris and Irwin (1985), and the expression for $S(\alpha)$ from Pastor et al. (1995). This latter expression is preferred to the more usual Srawley expression because it gives the correct limit for K_I for short cracks —i.e. 4.4 % less than the Srawley limit $1.12\sigma_N\sqrt{\pi a}$, as required by (3). Fig. 7a shows the resulting size effect curve. Note that there is a descending branch for small sizes, which is unrealistic.

To compare the rupture moduli predicted by the Jenq-Shah model with the cohesive model, we again force the asymptotic behavior to coincide. Taking two terms of the power expansion of functions $S(\alpha)$ and $M(\alpha)$ one easily finds the asymptotic Jenq-Shah prediction is

$$\frac{f_r}{f_0} \approx 1.049\left(1+\frac{1}{5.3D/\ell_0}\right) \tag{24}$$

which can be made to coincide with the first order approximation of the cohesive crack in (13)-(14) —with $\beta = 1.046$— if we set

$$f_0 = 0.997 f_t \approx f_t\,, \qquad \ell_0 = 2.3\,\ell_1 \tag{25}$$

An analytical expression with the correct asymptotic limit has been fitted to describe the prediction for sizes $D > \approx 0.15\,\ell_0$. The expression, drawn as a dashed line in Fig. 7a, is as follows:

$$\frac{f_r}{f_0} = 1.049\left(1+\frac{6.1D/\ell_0}{(1+6.1D/\ell_0)(1+5.3D/\ell_0)}\right) \tag{26}$$

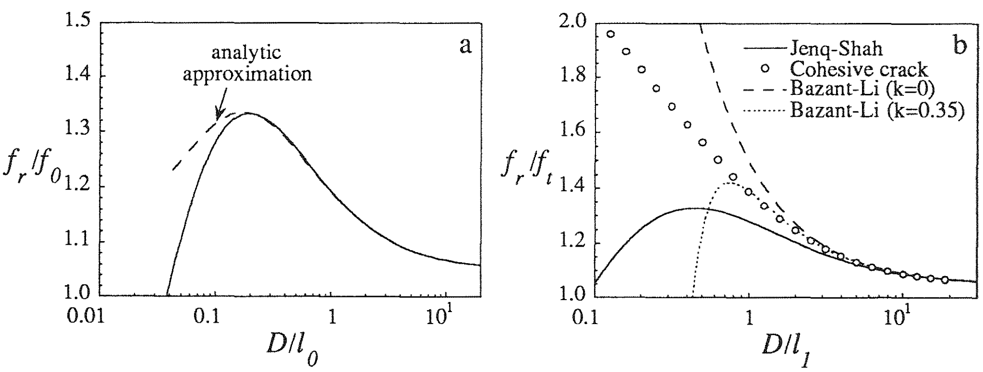

Fig. 7. Size effect curve for the modulus of rupture according to Jenq–Shah two parameter model.

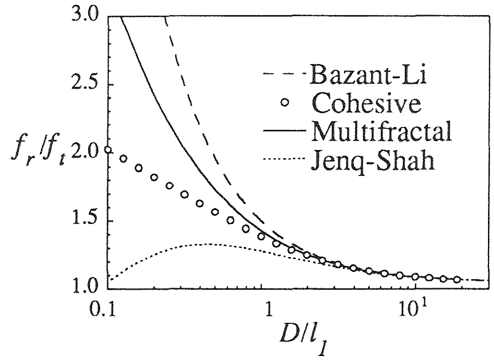

Fig. 8. Comparison of the multifractal scaling law with the other theories for identical asymptotic behavior.

4.3 Carpinteri's multifractal scaling law

Recently, a scaling law for strength based on the consideration of the fractal nature of the fracture process has been put forward by Carpinteri, Chiaia and Ferro (1994). This so called multifractal scaling law provides a continuous transition from the macroscopic scale in the large size range —fractal dimension equal to 1— to the microscopic fully disordered limit, in which the theoretical dimension is 1/2. The multifractal scaling law can be written in the following way:

$$\frac{f_r}{f_t} = \beta\sqrt{1 + \frac{\ell_M}{D}} \tag{27}$$

where f_t is the tensile strength in the macroscopic limit (large size) and ℓ_M is a constant length characteristic of the material and of the geometry. We introduce the factor β to provide consistency with the other theories.

In order to compare with the other theories, we again make the asymptotic expressions to coincide. The result is now

$$\ell_1 = 1.15\ \ell_M \qquad \text{or} \qquad \ell_M = 0.87\ \ell_1 \tag{28}$$

Fig 8 shows that the multifractal law lies between the size effect curves deduced from the cohesive model and that corresponding to the Bazant-Li model.

5 Comparison with experiments and final remarks

In the foregoing analysis, the various models for size effect on the modulus of rupture were analyzed assuming that for large sizes they must predict identical behavior. This is possible because all models display the same asymptotic structure.

However, in practice the asymptotic limit is never reached and what is usually sought is the value of the parameters of the model based on

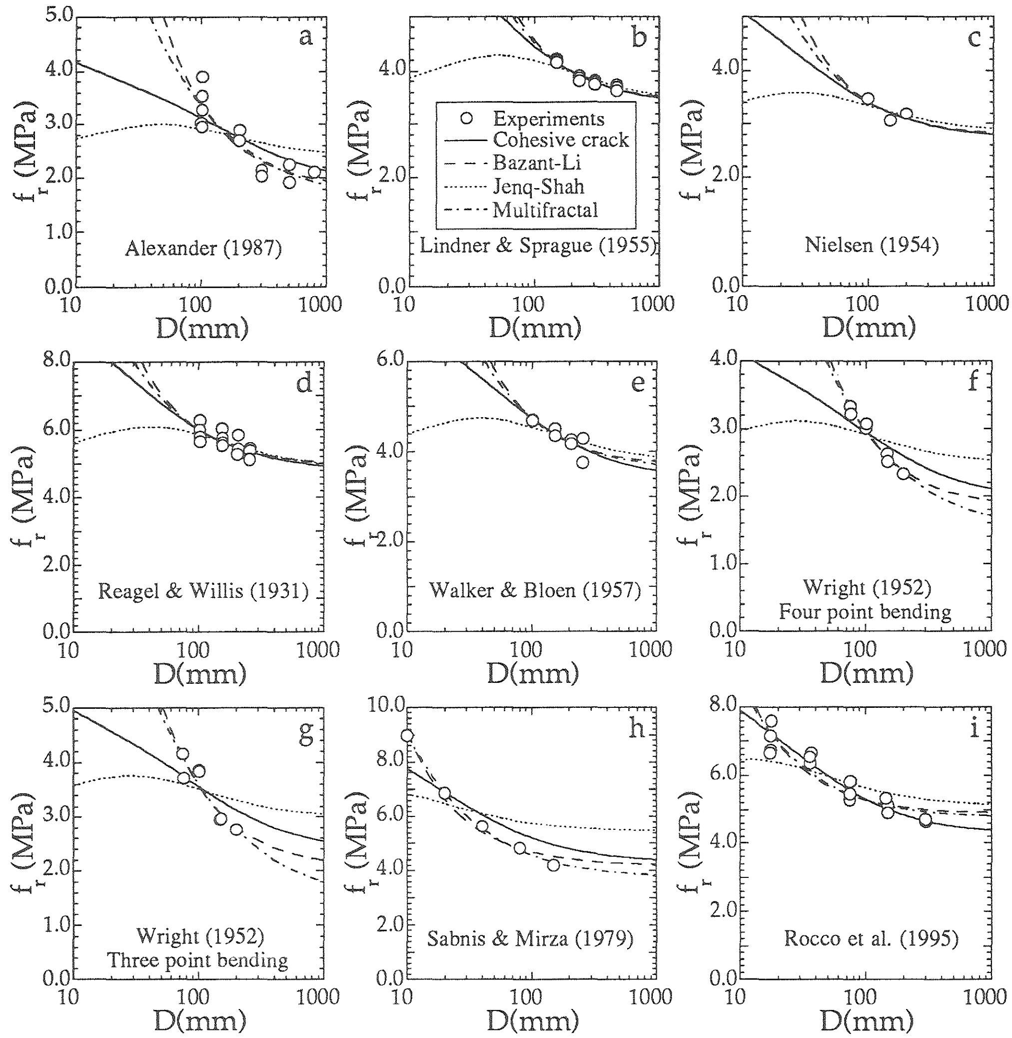

Fig. 9. Experimental results from various sources and best fits for the various models analyzed in the paper.

relatively small specimen results. Then the problems arise about the ability of the models to describe the results, on one hand, and of the ability of the results to select the best model.

Fig. 9 shows the experimental results from 9 experimental series and the theoretical curves found by nonlinear correlation assuming equally weighted data-points. Results *a–g* correspond to concrete, *h* to mortar, and *i* to microconcrete. It appears that the Jenq-Shah model is the one experiencing most difficulty in describing the experimental results, since only for series *b, c, d* and *e* are the slope of the experimental curve and of that model in relatively good agreement. The Bazant-Li and Multifractal fittings are essentially coincident for all experimental series. The cohesive, Bazant-Li and Multifractal models agree equally well with the experimental series *b, c, d* and *e*; the Bazant-Li and Multifractal models give better fits than the cohesive model for the series *a, f* and *g*; the cohesive model gives a better agreement for series *i*.

When all circumstances are taken into account it is difficult to conclude that any of the models is clearly superior to the others. Even if some of the cohesive crack predictions seem to be slightly less accurate than the Bazant-Li and Multifractal equations, the cohesive model has the advantage of being a very general fracture model that can be verified by independent tests, which is not possible for the other two models. Moreover, the cohesive crack can be extended to include statistical effects, a feature that, as shown by Gustafsson (1985), can make it fit very well the results showing a stronger size effect, such as those of Wright (1952) and Sabnis and Mirza (1979), series *f, g* and *h* in Fig. 9.

We therefore conclude with the following remarks:

1. The cohesive crack model provides a consistent framework for the analysis of the modulus of rupture. The results depend on only two material constants for initially linear softenings and can be conveniently summarized by Eq. (11). However, further work is required to incorporate secondary microcracking into the cohesive crack numerical algorithm. A deeper understanding of the statistical effects would also be of great interest.

3. The Bazant-Li model and Multifractal scaling law should be inserted in more general frameworks providing the means for independent determination of the basic fracture parameters.

4. The available experimental results are largely inconclusive regarding the predictive power of the models. Testing on a larger size range might help in strengthening the validation criteria, but much better would be to perform complementary tests providing independent determination of the basic fracture properties of the material.

Acknowledgments. The authors gratefully acknowledge support for this research provided by DGICYT and CICYT, Spain, under grants PB93-31 and MAT 94-120-C03.

6 References

Alexander, M. G. (1987) in Shah, S. P. and Ouyang, C. (1994) Fracture mechanics for failure of concrete. **Annu. Rev. Mater. Sci.** 24, 293–320.

Alvaredo, A. M. and Torrent, R. J. (1987) The effect of the shape of the strain-softening diagram on the bearing capacity of concrete beams. **Materials and Structures**, 20, 448–454.

Bazant, Z. P., Xi, Y., and Reid, S.G. (1991). Statistical size effect in quasi-brittle structures: I. Is Weibull theory applicable? ASCE **J. of Engineering Mechanics**,117(11), 2609–2622.

Bazant, Z. P. (1984). Size effect in blunt fracture: concrete, rock and metals. **J. Engrg. Mech. ASCE**, 110, 518–538.

Bazant, Z. P., and Li, Z. (1993). Modulus of rupture: size effect due to fracture initiation in boundary layer. Report No. 93-5/457m, Dept. of Civil Engineering, Northwestern University.

Carpinteri, A., Chiaia, B. and Ferro G. (1994) Multifractal scaling law for the nominal strength variation of concrete structures, in **Size Effect in Concrete Structures** (eds H. Mihashi, H. Okamura and Z. P. Bazant) , E & FN Spon, London, 193–206.

CEB-FIP (1990) **CEB-FIP Model Code For Concrete.**

Elices, M., Guinea, G. V. and Planas, J. (1994) Prediction of size effect based on cohesive crack models, in **Proc. IUTAM Symp. on Size Scale Effect in the Failure Mechanisms of Materials and Structures**. Torino, Italy, October 3–7 1994.

Eo, S. H., Hawkins, N. M. and Kono S. (1994) , in **Size Effect in Concrete Structures** (eds H. Mihashi, H. Okamura and Z. P. Bazant) , E & FN Spon, London, 245–254.

Gustafsson, P.-J. (1985) Fracture mechanics studies of non-yielding materials like concrete: modeling of tensile fracture and applied strength analyses. Report TVBM-1007, Division Building Materials, Lund Institute of Technology, Lund, Sweden.

Hillerborg, A., Modéer, M. and Petersson, P.-E. (1976) Analysis of crack formation and crack growth in concrete by means of fracture mechanics and finite elements. **Cem. Concr. Res.**, 6, 773–782.

Jenq, Y. S., and Shah, S. P. (1985) Two Parameter Fracture Model for Concrete. **J. of Engng. Mech.**, ASCE, 111, No. 10, pp. 1227–1241.

Kellerman, W. F. (1932) Effect of size of specimen, size of aggregate and method of loading upon the uniformity of flexural strength tests. **Public Roads**, 13, 177-184.

Lindner, C. P., and Sprague, I. C. (1955) Effect of depth of beams upon the modulus of rupture of plain concrete. **ASTM Proc.**, 55, 1062–1083.

Modéer, M. (1979) A fracture mechanics approach to failure analyses of concrete materials. Report TVBM-1001, thesis, Div. of Building Mat., Univ. of Lund, Sweden.

Nielsen, K. E. C. (1954) Effect of various factors on the flexural strength of concrete test beams. **Magazine of Concrete Research**, 15, 105-114.

Olsen, P. C. (1994) Some comments on the bending strength of concrete beams. **Magazine of Concrete Research**, 46, 209–214.

Pastor, J. Y., Guinea, G., Planas, J. and Elices, M. (1995) Nueva expresión del factor de intensidad de tensiones para la probeta de flexión en tres puntos. **Anales de Mecánica de la Fractura**, 12, 85–90. ("A new expression for the stress intensity factor of a three-point bend specimen," in Spanish.)

Petersson, P.-E. (1981) Crack growth and development of fracture zone in plain concrete and similar materials. Report TVBM-1006, Division of Building Materials, Lund Institute of Technology, Sweden.

Planas, J. and Elices, M. (1992) Shrinkage eigenstresses and structural size-effect, in **Fracture Mechanics of Concrete Structures** (ed Z. P. Bazant) Elsevier Applied Science, London, 939–950.

Planas, J. and Elices, M. (1993) Drying shrinkage effect on the modulus of rupture, in **Creep and Shrinkage of Concrete** (eds Z.P. Bazant and I. Carol) E & FN Spon, London, 357–368.

Reagel, F. V. and Willis, T. F. (1931) The effect of dimensions of test specimens on the flexural strength of concrete. **Public Roads**, 12,37-46.

Rocco, C., Guinea, G. V., Planas, J. y Elices, M (1995) Variación del módulo de rotura de un microhormigón con el tamaño de las probetas. Report 95cr02, Dep. Ciencia de Materiales, ETSI Caminos, UPM, Madrid, Spain.

Rokugo, K., Iwasa, M., Suzuki, T. and Koyanagi, W. (1989) Testing methods to determine tensile strain softening curve and fracture energy of concrete, in **Fracture Toughness and Fracture Energy. Test Methods for Concrete and Rock** (eds H. Mihashi, H. Takahashi and F. H. Wittmann), Balkema, Rotterdam, 153-163.

Tada, H., Paris, P. and Irwin, G. (1985) **The Stress Analysis of Cracks Handbook**, Del Research Corporation.

Timoshenko, S. and Goodier, J. N. (1951) **Theory of Elasticity**. McGraw-Hill, New York.

Uchida, Y., Rokugo, K. and Koyanagi, W. (1992) Application of Fracture Mechanics to Size Effect on Flexural Strength of Concrete. **Proc. JSCE**, 16, 101–107.

Walker, S. and Bloen, D. L. (1957) Studies of flexural strength of concrete—Part 3: Effects of variations in testing procedures. **ASTM Proc.**, 57, 1122-1139.

Weibull, W. (1939). A Statistical Theory of the Strength of Materials. **Proc. Royal Swedish Academy of Eng. Sci.** , 151, 1–45.

Wright, P. J. F. (1952) The effect of the method of test on the flexural strength of concrete. **Magazine of Concrete Research**, 11, 67-76.